



Conference Proceedings Paper – Remote Sensing

MODIS-Landsat Data Fusion for Estimating Vegetation Dynamics – A Case Study for Two Ranches in Southwestern Texas

Di Yang¹, Hongbo Su^{2,*}, Yan Yong², Jinyan Zhan³

1 Department of Geography, University of Florida, USA; E-Mails: yangdi1031@gmail.com (D.-Y);

2 Department of Civil, Environmental and Geomatics Engineering, Florida Atlantic University, USA

3 State Key Laboratory of Water Environment Simulation, School of Environment, Beijing Normal University, Beijing 100875, China; E-Mails: zhanjy@bnu.edu.cn

* Author to whom correspondence should be addressed; E-Mail: suh@fau.edu;
Tel.: +1-561-297-3936.

Published: 6 June 2015

Abstract: Remote sensing has been widely used in vegetation-dynamics monitoring. Many studies have used data acquired by multispectral sensors, such as the Landsat TM sensor, due to their high spatial resolution (30 m). However, during the growing season, the temporal resolution (16 day) cannot capture rapid changes of vegetation. Meanwhile, coarse-spectral-resolution sensors, such as Moderate Resolution Imaging Spectroradiometer (MODIS), have high-frequency temporal information that can catch the details of landscape changes. In this research, we proposed a data-fusion approach to merge the MODIS and Landsat TM data to create a dataset of vegetation dynamics with both a high spatial resolution and a fine temporal resolution. The Comanche and Faith Ranches, located in west Texas, were chosen for this study. The MODIS product was used as a regionally consistent reference dataset to correct the Landsat imagery. Based on this new dataset, NDVI time-series curves from 2004 to 2011 were calculated with the MODIS 13 Vegetation Dataset. One random sample of red-band images was tested and compared with MODIS data. A high correlation coefficient 0.907 and RMSE 0.0245 was found.

Keywords: Data fusion; Vegetation Dynamics; Landsat TM; Moderate Resolution Imaging Spectroradiometer (MODIS); Normalized Difference Vegetation Index (NDVI); Surface reflectance

1. Introduction

Data fusion is the process of combining information from heterogeneous sources into a single composite picture of the relevant process, such that the composite picture is generally more accurate and complete than can be derived from a single source alone [1]. Spatial and temporal remote-sensing data fusion is a technique that can produce a dense time-series database with a high spatial resolution [2]. In this database, the temporal resolution is the same as the high-temporal-resolution data and the spatial resolution fits with the high-spatial-resolution database. With the aid of time-series data fusion, changes in land surface, such as vegetation dynamics, can be easily detected and monitored. Time series of Vegetation indexes (VIs), such as the Normalized Difference Vegetation Index (NDVI) and the Enhanced Vegetation Index (EVI), represent land-surface vegetation dynamics in both time and space [3]. These time series are generally derived from a multi-temporal, coarse-spatial-resolution data set. However, when the study area is small in scale, issues of vegetation-monitoring dynamics arise with the pixel size of the coarse imagery [4]. In this situation, if the study areas focus on medium- or low-vegetation analyses (such as grasses and shrubs); a database of analyses in high temporal and spectral resolution is critical. Coarse-spatial-resolution sensors (from 250 m to a few kilometers) such as MODIS, NOAA, SPOT VEGETATION, and MERIS commonly have relatively high temporal resolution (such as daily) [5]. On the contrary, the medium- and low-spatial-resolution sensors, such as Landsat TM, could detect most of the vegetation variations, but lack temporal resolution. In many cases, it is very hard to get a rapid response to vegetation dynamics [6].

Currently, the available satellite data set, which is limited by spatial and temporal characteristics, influences the accuracy of mapping land cover at a continental scale [7,8]. Corresponding with the Landsat TM sensor, MODIS has close solar geometries and orbital parameters. This would enable the fusion of Landsat TM and MODIS time-series data by subpixel in both time and space. A data-fusion approach can therefore be designed by combining the daily MODIS 250 m surface-reflectance product (MODIS09GQ) [9] with Landsat data in order to generate a modeled “daily” Landsat data set. The modeled data product can keep a fine spatial resolution (30 m) to capture the land cover in details, and can keep high temporal resolution (daily) to accurately determine changes over time [8].

In recent years, scholars around the world have developed advanced research and methods on time-series data fusion [4,8,19,20]. Most methods are based on linear-mixed models and assume no changes in surface reflectance by pixel in the same category. Due to the influence of geologic environments, there are reflectance changes in surface features in space. Some scholars proposed improved algorithms based on the assumption that there are no dramatic changes in the neighborhood pixels [4,8,21]. The evaluation of the methods has been applied in many fields such as dry-land forest phenology [10] [11], and forest-cover changes [12–14].

Landsat TM sensors, with a high spatial resolution of 30 m and a 16-day revisit cycle, are widely used for mapping a range of biophysical vegetation parameters and monitoring regional land cover [15]. In the past 30 years, Landsat data have been used to gather ecological information such as the

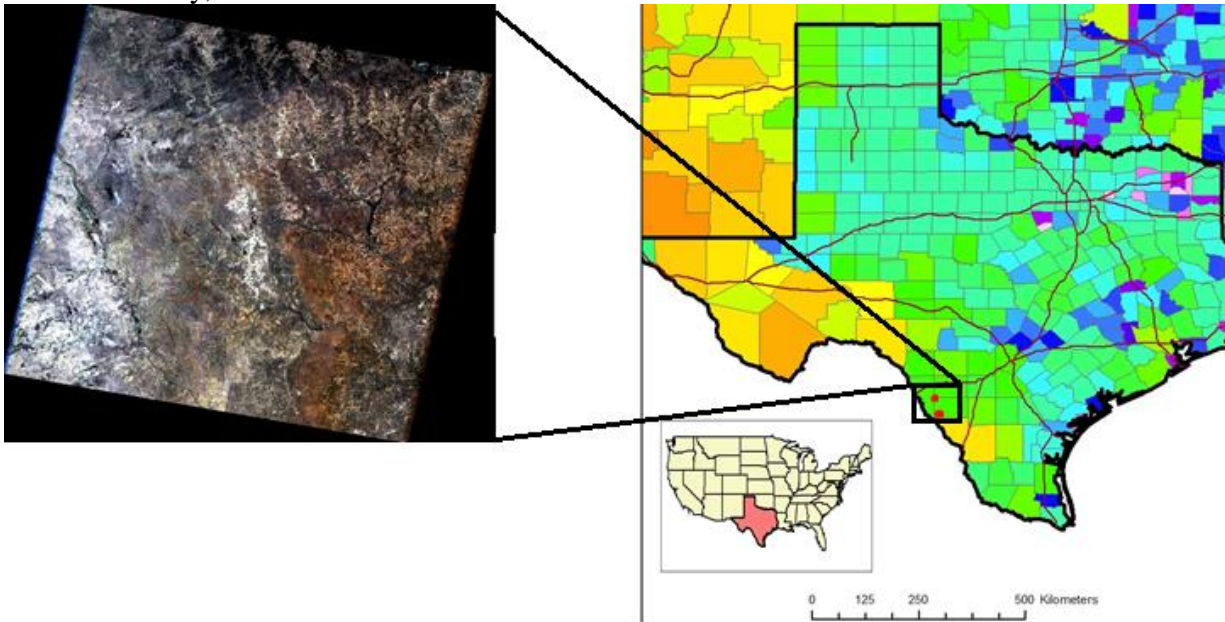
dynamics of ecosystems and the detection of changes in land cover [16], and as an efficient tool for monitoring vegetation-cover changes in tropical-forest domains [17]. However, the applications of Landsat data in monitoring biodynamic and surface changes are limited due to cloud contamination and a 16-day minimum TM-sensor revisit cycle. Cloud contamination can lower data quality and cause missing data. During data acquisition, clouds covering and lowering temporal resolution could be the major obstacle for monitoring changes in vegetation characteristics in the study area. NASA's Moderate Resolution Imaging Spectroradiometer (MODIS) provides vital information and high-quality-data resources for land cover research [18]. With a lower spatial resolution (250 m, 500 m and 1,000 m), MODIS Terra/Aqua revisit the globe multiple times per day.

The research strategy engaged herein focuses on linear-pixel decomposition [22]. We extracted the time curve of surface reflectance based on a high temporal-resolution data set. After combining it with the high-spatial-resolution data, we got a database with high resolutions in both time and space. In this study, two ranches (Faith Ranch and Comanche Ranch) in west Texas were chosen for the study areas. Images from the MODIS daily surface-reflectance product (MOD09GQ) and Landsat TM 5 from 2004-2011 were chosen to build the new data set and evaluate the fusion results. The NDVI time-series data set was produced by the modeled-fusion result. This method is automated and greatly shortens computation time.

2. Study Area

The study areas are the Faith Ranch (28.613N; -100.092W) and Comanche Ranch (28.381N; -100.009W) located in Dimmit County in west Texas. The dominant vegetation type is shrubs with grass, principle habitat for white-tailed deer. The most notable feature of the study area is the plain. Site records indicate the area of Faith and Comanche ranches are 5,028km² and 4,855km², respectively, with an annual inter variability of precipitation between 448.6 mm and 463.9 mm per year. Each ranch had 6 equal-area enclosures for experiments, which can be easily distinguished by Landsat TM data. The distance between the two ranches is 37 km; however, 250-m MODIS09 imagery resolution is not sufficient to detect changes in vegetation dynamics in these areas.

Figure 1. Landsat 5 TM Satellite Maps and Location of Study Area, Comanche and Faith Ranches in Dimmit County, Texas



3. Methodology

3.1 Methods

The data-fusion method in this study is designed to capture high-resolution spatial changes from Landsat TM 5 data, while the high temporal resolution of MODIS 09 imagery is used to accurately determine the occurrence time of a given disturbance. The inputs of this method are: 1) two adjacent Landsat TM 5 images (one at the beginning of the period and the other is at the end), and 2) MODIS surface-reflectance images at a given date in the measurement period.

Cloud contamination tends to reduce reflectance in the near-infrared band and increase it in the red band, thus the ratio value of the vegetation indices fluctuates heavily. When the cloud cover is greater than 10%, the probability of acquiring good quality Landsat imagery can be as low as 10% regionally [23].

For each homogenous pixel at MODIS resampled data, the relationship of the surface reflectance measured by Landsat TM sensor can be represented as:

$$L_{(x_i, y_i, t_k)} = M_{(x_i, y_i, t_k)} \times \xi_k \quad (1)$$

where t_k is the Landsat and MODIS data acquisition date, $L_{(x_i, y_i, t_k)}$ is the surface reflectance of the calibrated Landsat imagery at a given location (x_i, y_i) . At the same pixel location, $M_{(x_i, y_i, t_k)}$ is the previously geo-referenced and resampled MODIS surface reflectance. In the equation, ξ_k represents the conversion factor between the two sensors (caused by different solar-elevation angle and bandwidth settings). Here it is assumed that the MODIS surface reflectance $M_{(x_i, y_i, t_k)}$ has been geo-referenced and resampled to the resolution and bounds of the Landsat surface reflectance image $L_{(x_i, y_i, t_k)}$ and thus shares the same pixel size, coordinate system, and the image size.. From the geographical space, we suppose that in a comparatively short period of time (such as one day), changes

in surface reflectance are continuous, which means the land cover will not change radically in that short period of time.

Similarly, at the data of t_0 , the relationship between Landsat and MODIS sensors surface reflectance can be expressed as:

$$L_{(x_i, y_i, t_0)} = M_{(x_i, y_i, t_0)} \times \xi_0 \quad (2)$$

Supposing there are no changes in cover types or systematic errors from date t_0 to t_k , meaning $\xi_0 = \xi_k$. After combining equation (1) and (2), equation (3) can be written as:

$$\frac{L_{(x_i, y_i, t_k)}}{L_{(x_i, y_i, t_0)}} = \frac{M_{(x_i, y_i, t_k)}}{M_{(x_i, y_i, t_0)}} \quad (3)$$

Under ideal conditions, the surface reflectance of Landsat at date t_k at a given pixel (x_i, y_i) is: surface reflectance of Landsat at date t_0 multiplied by the ratio of MODIS surface reflectance between date t_k and t_0 . However, the ideal modeled relationships between MODIS and Landsat surface reflectance do not fit the equation all the time.

$$L_{\left(\frac{x_w}{2}, \frac{y_w}{2}, t_0\right)} = \sum_{i=1}^w \sum_{j=1}^w \sum_{k=1}^w w_{ijk} \times \left(\frac{M_{(x_i, y_i, t_0)}}{M_{(x_i, y_i, t_k)}} \times L_{(x_i, y_i, t_k)} \right) \quad (4)$$

In the equation, where the $\left(\frac{x_w}{2}, \frac{y_w}{2}\right)$ is the central pixel of the sliding window, $L_{\left(\frac{x_w}{2}, \frac{y_w}{2}, t_0\right)}$ is the surface reflectance to be predicted on date t_0 , w is the size of window (only valid pixels are used for prediction in the windows). $M_{(x_i, y_i, t_0)}$ and $M_{(x_i, y_i, t_k)}$ are the pixel values of MODIS data on the date t_0 and t_1 , respectively. The weight coefficient herein is introduced: the weight " w_{ijk} " determines the contributions from each neighbor pixel to the estimated reflectance of the central pixel. In the process of prediction, the problem can be resolved by introducing the sliding window concept to minimize the boundary influence.

During central-pixel value calculation, the weight w_{ijk} depends on three main factors: 1) spectral difference, 2) time-information difference, and 3) space-relative distance. The weight can be expressed as:

$$w_{ij} = (1/C_{ij}) / \sum_{i=1}^w \sum_{j=1}^w (1/C_{ij}) \quad (5)$$

where C_{ij} is the value, which combines the predicted central pixel with the rest of the pixels in the sliding window, considering the three main factors (spectral difference, time-information difference, and space-relative distance). All images used in this study were clipped based on the region of interest (ROI) of the Comanche Ranch and Faith Ranch. Regions of interests (ROIs) of the two ranches were built to calculate the NDVI, respectively.

3.2. Data Processing

3.2.1 Landsat-5 TM Data Set

Landsat 5 TM data were acquired from January 2004 to November 2011. All data sets have high data quality and are cloud-cover free. The Landsat TM sensor onboard the Landsat 5 platform has a spatial resolution of 30 m and a spatial extent of 185×185 km per scene, which is well suited for characterizing landscape-level forest structure and dynamics. Arguably, Landsat is the most commonly

used satellite sensor for mapping biophysical vegetation parameters and land cover [7]. Landsat images have advantageous spatial and spectral characteristics for describing vegetation properties; the temporal resolution for the Landsat TM 5 sensor is 16 days.

The 30 m Landsat pixel is adequate for mapping major vegetation changes [24], but the integration of high-temporal-resolution data allowed for a more detailed characterization of the landscape. The 16-day revisit cycle is often extended due to cloud contamination or duty cycle limitations [25]. Cloud cover is a major obstacle for monitoring short-term disturbances and changes in vegetation characteristics through time. Moreover, the probability of acquiring cloud-free Landsat imagery for a given year (cloud cover below 10%) can be as low as 10% [23]. In the cloudy area of the Earth, the problem is compounded, and researchers are fortunate to get two to three clear images per year.

3.2.2 MODIS 09 Surface Reflectance Data Set

Datasets from the Moderate Resolution Imaging Spectroradiometer (MODIS) sensor onboard NASA's Terra and Aqua satellites are imaged daily at the global scale, providing the best possibility of cloud-free observations from the platform. Conversely, high-temporal-resolution sensors have a more frequent revisit rate and produce wide-area coverage with a lower spatial resolution [26]. The Terra/Aqua MODIS satellites provide frequent coarse-resolution images, revisiting the earth's surface at least once per day. Bands 1-7 of MODIS images were designed primarily for remote sensing of land surface, including: blue band (459 to 479 nm), green band (545 to 565 nm), red band (620 to 670 nm), near infrared band (841 to 876 nm), and the mid-infrared band (1230 to 1250nm, 1628 to 1652nm, 2105 to 2155 nm). The red and the near-infrared (NIR) bands were used to map NDVI in this project. To match the bandwidths with the Landsat TM sensor, a comparison of bandwidth between the Landsat TM sensor and the MODIS sensor is shown below:

Table 1. Landsat TM and MODIS Bandwidth [8]

Landsat TM Band	TM Bandwidth (nm)	MODIS Band	MODIS Bandwidth (nm)
1	450 - 520	3	459 - 479
2	530 - 610	4	545 - 565
3	630 - 690	1	620 - 670
4	780 - 900	2	841 - 876
5	1550 - 1750	6	1628 - 1652
7	2090 - 2350	7	2105 - 2155

Depending on the spectral characteristics of interest, MODIS dataset have spatial resolutions of 250 m, 500 m, and 1000 m. However, at the same time, the coarse resolution of MODIS limits the sensor's ability to quantify biophysical processes in heterogeneous landscapes.

MODIS data were downloaded from the Earth Observing System Data Gateway distributed archive (<http://reverb.echo.nasa.gov/reverb/>). MODIS images were reprojected to the UTM 84 Datum and resized separately for the two ranches in the study area by an Arcmap shape file. The data set was composed of 2,703 daily 250 m surface-reflectance images (Product MOD09GQ-V005) acquired at the same time as the TM images, and 23 250 m, 16-day MODIS-NDVI composite images covering January 2004 to November 2011 (Product MOD13Q1-V004) [27]. All MODIS products were

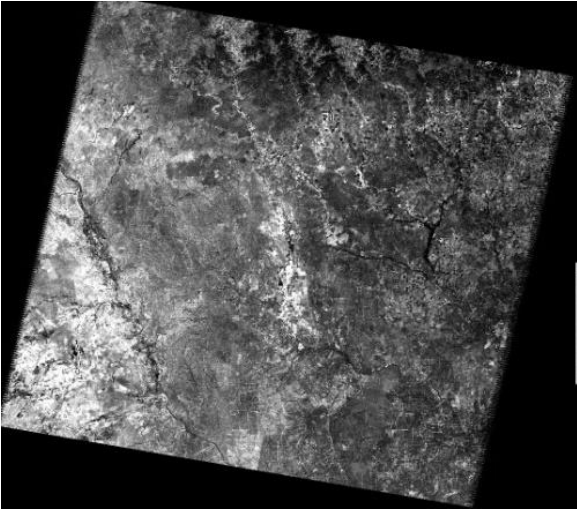
automatically transformed to a GEO-TIFF format with a MODIS Reprojection Tool (MRT) and resampled to 30 m Landsat-imagery resolution by using the nearest-neighbor method. Red and NIR bands in the MODIS data were extracted, respectively. The data set included extensive quality control (QC) information to exclude cloud contamination and take care of data-processing conditions.

4. Results

In this section, we analyzed the algorithm performance over the two example ranches (Faith and Comanche ranches) in west Texas. The performance of the approach is evaluated by statistically comparing the experimental results (MODIS original data) with model estimates of time-series maps of the two ranches using the method in this study. Meanwhile, red and NIR bands were chosen to be modeled in this study for convenience of computer programming and for calculating NDVI (by the equation $NDVI = (\text{Red Band} - \text{NIR Band}) / (\text{Red Band} + \text{NIR Band})$). As inputs, we used the red NIR bands from 30 m Landsat TM 5 data that were 90% cloud free, and 250 m MODIS 09 surface-reflectance data, both red and NIR bands, from 2004 to November 2011. For final outputs, we got the data set with a spectral resolution of 30 m and the temporal resolution of once daily with both the red and NIR bands modeled. The composed data set has high quality in both red and NIR bands. Figure 2 shows a random example of the fusion result of a period from Jan. 21, 2011 to Feb. 5, 2011. The input data are surface-reflectance red band of Landsat TM 5 from Jan. 21, 2011 and Feb. 5, 2011, and one MODIS red-band image from Jan. 21, 2011, which has the same data as the first Landsat data. The outputs of the processing are daily images with space resolution of 30 m during the test period from Jan. 21, 2011 to Feb. 5, 2011, respectively.

IDL language programming was used to produce Landsat-MODIS time-series maps from 2004 to 2011 of the Comanche and Faith ranches in Texas. These models are going to run automatically after obtaining the direction of the input data set. We tested the result-pixel images for the Comanche Ranch, the area of which is 4,855 km², on the acquired date of Feb. 5, 2011. All images used in this study were clipped based on the region of interest (ROI) of the Comanche Ranch and Faith Ranch. ROIs were built based on shape files of the two ranches, respectively. The NDVI maps of the Comanche Ranch of a different model than mentioned here are shown in Figure 3.

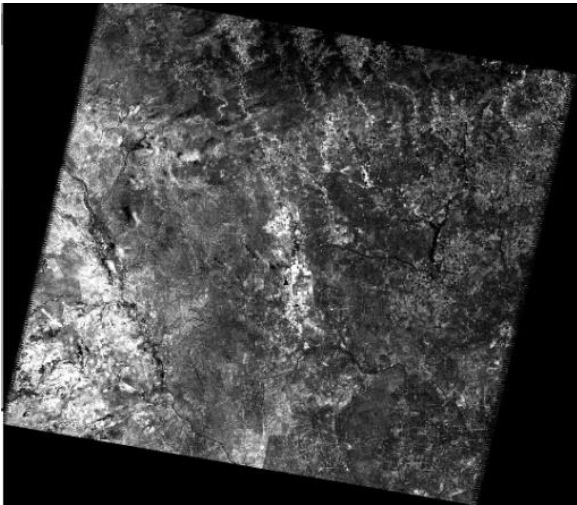
Figure 2. Prediction of surface reflectance (red band) from MODIS imagery and Landsat imagery



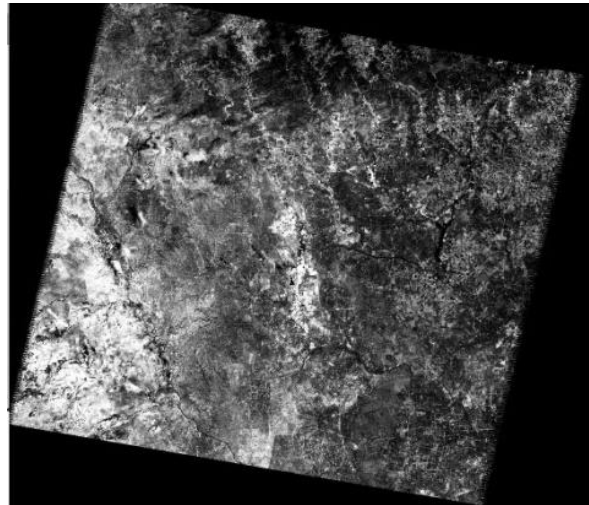
Landsat 1/21/2011



MODIS 1/21/2011

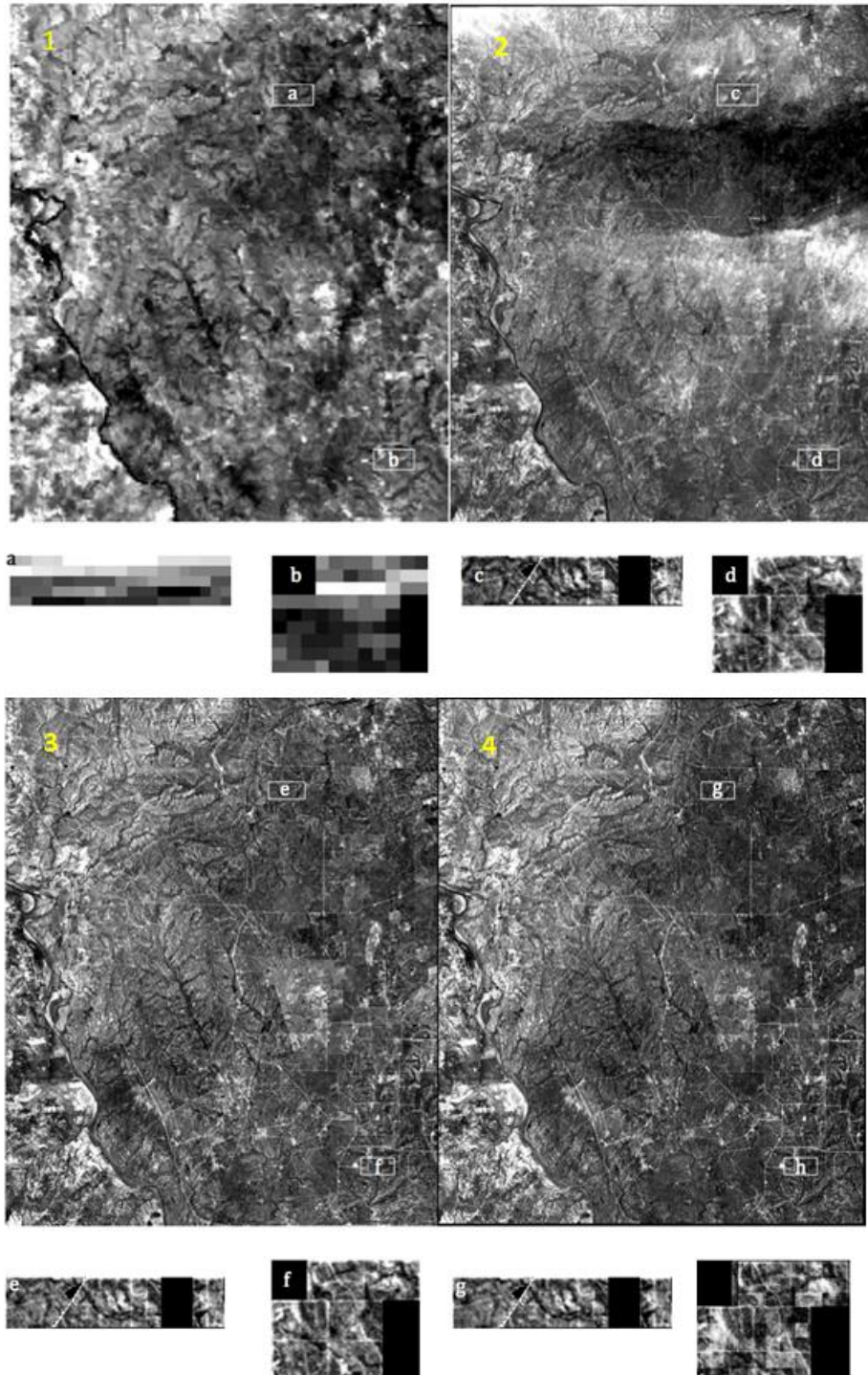


Landsat 2/5/2011



Predict Date: 1/22/2011

Figure 3. Combination of MODIS and Landsat TM images: **(a)&(b)** original low-resolution MODIS09 image in Band 1 of Faith and Comanche Ranch, respectively; **(c)&(d)** high-resolution Landsat TM image in red Band of Faith and Comanche Ranch, respectively; **(e)&(f)** reference high-resolution Landsat TM image in Band 3 of Faith and Comanche Ranch; **(g)&(h)** Modeled image of Faith and Comanche Ranches after the fusion of MODIS and Landsat TM images.

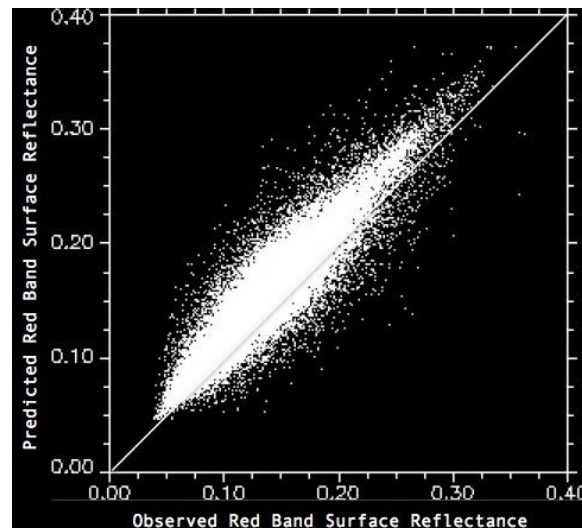


The study method was run in IDL programming by bands. The red and near-infrared (NIR) bands were chosen for modeling to make a time-series dataset product. The process of combining MODIS and Landsat TM images for the Faith and Comanche ranches is illustrated in Figure 3. It shows that one of the low-resolution MODIS images (Jan. 21, 2011) and two high-resolution Landsat TM images (Jan. 21, 2011 and Feb. 5, 2011) were used to obtain a new of high-resolution, time-series data set. Because the correlation coefficients represent the degree of similarity between the original satellite image and the modeled image, we used the correlation coefficients to evaluate the modeled results of the database.

In Figures 3 and 4, there is a slight difference that could be indistinct between the Landsat-band map and modeled-band map. Even after transmitting the modeled data to the NDVI map after calculating the combination of red and NIR bands, there are still great correlation coefficients; RMSE is 0.02453, and 55,876 points are calculated in total. Figure 4 shows a 2D scatter plot of the modeled fusion band 1 versus the high accuracy MODIS data at the date of Sep 12, 2011. The modeled data indicates a very high correlation with the high-quality MODIS data, with $R^2 = 0.907$.

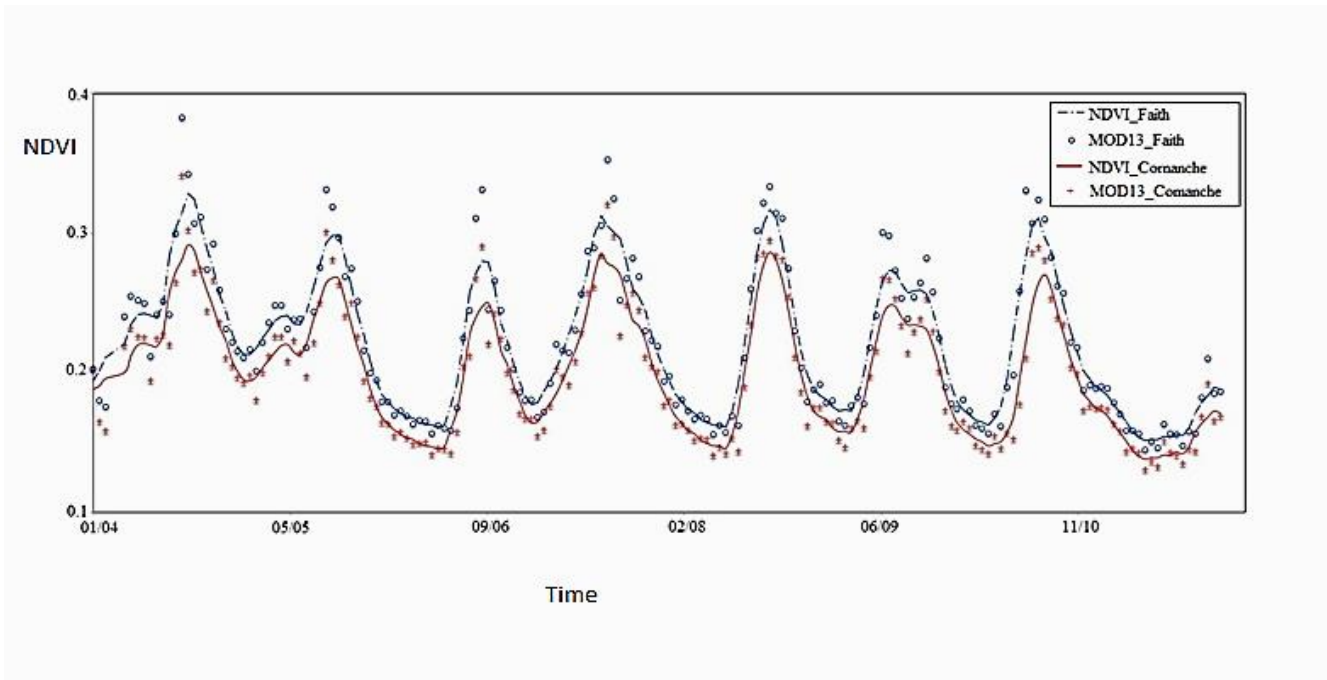
Figure 4. Cross-validation plot for the Landsat Surface Reflectance Model. $R^2=0.907$

and RMSE = 0.02453



The MODIS 13 NDVI map dataset was employed in this study, and the MODIS 13 vegetation products are available every 16 days with a spatial resolution of 250 m. Due to providing the best possibility for cloud-free observation because of its polar-orbiting platform, MODIS 13 vegetation products became the ideal reference standard for the fusion results. Based on the band-math method, we built up a new dataset by calculating the NDVI with modeled results from red and NIR bands. NDVI values of the modeled dataset were computed from red in NIR surface reflectance for each daily image. After the comparison with MODIS 13 data, we found there is still a high correlation between the new database and the high-quality MODIS 13 data. Figure 5 shows the comparison between MODIS 13 NDVI layer data and modeled band math NDVI data from 2004-2001 at the two ranches, respectively.

Figure 5. Comparison of MODIS 13 NDVI data and modeled NDVI data from the year of 2004-2001 at the Faith and Comanche ranches



5. Discussion

Table 2 shows the comparison of the method in this study with STARFM and other multisensor-fusion methods. The results indicate the method we developed in this study has an equivalent or higher correlation coefficient. The main characteristics are: 1) both before (t_0) and later (t_k) high-resolution images were used to produce the data-fusion data set with more texture information in details; 2) this new database has a high correlation with the high-temporal-resolution images (MODIS), and the high currency from the high-temporal database was kept in the new fusion database that we got in the study; 3) the new database considerably reduced the running time of data-fusion processing, facilitating the establishment of a relatively long time-series data set, even 10 years or more; 4) the new database has good pixel fidelity, and the resolution of the data-fusion dataset is a measure of the fidelity of pattern transfer. When the study area focuses on a small area, such as the two ranches in this study, we still have great fitness in the zoom-in pixel maps.

Table. 2 Comparison between currently different time series fusion methods

Objective	Sensors	Correlation Coefficient	RMSE	Method
NDVI	MODIS and Landsat TM	0.78-0.89	0.07-0.105	Busetto 2008
Reflectance	MODIS and Landsat TM	0.91	0.02-0.06	Thomas 2009

Meanwhile, fusion results are still influenced by the following factors: 1) systematic errors between different sensors. There are small biases in different sensor systems due to the differences in acquisition time, bandwidth ranges and data processing. 2) Linear-mixed modeling. The linear-mixed

model was adopted in the most of the multisensor time-series data-fusion methods. In this model, the linear-mixed model is perfect for the bare earth, or snow cover. However, when the land surface is covered with low vegetation or even forest, the sensors just get part of the reflection. The other part of the reflection is disturbance from the land-cover object. Therefore, the phenomena of nonlinear mixture are widespread.

In addition, the surface reflectance of invariant targets should remain relatively consistent over time. Atmospheric noise makes a huge contribution to variable reflectance errors over time. The dataset was preprocessed with the atmospheric correction because the atmospheric correction is able to minimize variance. There was no additional correction applied to the data to correct the view angle and reduce atmospheric and terrain effects.

6. Conclusions

By using a new fusion technology of spatial-temporal, remote-sensing data combining Landsat TM imageries with temporal MODIS surface-reflectance products, we produced a product that could have considerable utility for applications that require both high spatial resolution and frequent coverage (high temporal resolution). The modeled results were used to evaluate the vegetation dynamics of the Faith and Comanche ranches in west Texas. We confirmed the precision of the algorithm in this study through pixel-correlation analysis between high accuracy MODIS imagery and the modeled-fusion imagery.

High temporal and spectral resolution with a high accuracy time-series “Landsat” data set is achieved in this method; the correlation coefficient is higher than 0.9. The high correlation between the original data and the modeled data makes a great contribution to the assumption that we made about the time-series changes in a relatively short time. We also used the band math to get a new NDVI dataset based on the fusion result, and found that there is still a high correlation between MODIS 13 data and the modeled data.

In contrast to traditional multisensor-fusion methods, this method can be used to monitor vegetation dynamics without the land-cover maps and in-situ measurements. Due to the high temporal MODIS data, dataset temporal resolution can be greatly increased (at least one modeled data set per day in this study) so it is much easier to detect variances in vegetation dynamics.

Acknowledgments

Special thanks are given to Drs. David Hewitt and Timothy Fulbright for sharing the ideas of inspiration to study the vegetation dynamics over the ranches.

Author Contributions

Di Yang proposed and developed the research design, manuscript writing and results interpretation. Hongbo Su supervised all the work that has been done by the first author and revised the manuscript extensively. Yan Yong and Jinyan Zhan revised the manuscript.

Conflict of Interest

The authors declare no conflict of interest.

References and Notes

1. David David Lee Hall.; Sonya Anne Hall McMullen. Fusion Applications. *In Mathematical Techniques in Multisensor Data Fusion*, 2nd Ed; Publisher: Artech Print on Demand, USA, **2004**; pp. 3-13.
2. Wu, M. Spatial and Temporal Fusion of Remote Sensing Data Using Wavelet Transform. *2011 International Conference on Remote Sensing, Environment and Transportation Engineering* **2011**, 1581–1584.
3. Yang, P.; Shibasaki, R.; Wu, W.; Zhou, Q.; Chen, Z. Evaluation of MODIS Land Cover and LAI Products in Cropland of North China Plain Using In Situ Measurements and Landsat TM Images. **2007**, *45*, 3087–3097.
4. Busetto, L.; Meroni, M.; Colombo, R. Combining Medium and Coarse Spatial Resolution Satellite Data to Improve the Estimation of Sub-pixel NDVI Time Series. *Remote Sensing of Environment* **2008**, *112*, 118–131.
5. Hwang, T.; Song, C.; Bolstad, P. V.; Band, L. E. Downscaling Real-time Vegetation Dynamics by Fusing Multi-temporal MODIS and Landsat NDVI in Topographically Complex Terrain. *Remote Sensing of Environment* **2011**, *115*, 2499–2512.
6. Viña, A.; Bearer, S.; Zhang, H.; Ouyang, Z.; Liu, J. Evaluating MODIS Data for Mapping Wildlife Habitat Distribution. *Remote Sensing of Environment* **2008**, *112*, 2160–2169.
7. Liu, W.; Wu, E. Y. Comparison of Non-linear Mixture Models: Sub-pixel Classification. *Remote Sensing of Environment* **2005**, *94*, 145–154.
8. Masek, J.; Schwaller, M.; Hall, F. On the Blending of the Landsat and MODIS Surface Reflectance: Predicting Daily Landsat Surface Reflectance. *IEEE Transactions on Geoscience and Remote Sensing* **2006**, *44*, 2207–2218.
9. Justice, C. .; Townshend, J. R. .; Vermote, E. .; Masuoka, E.; Wolfe, R. .; Saleous, N.; Roy, D. .; Morisette, J. . An Overview of MODIS Land Data Processing and Product Status. *Remote Sensing of Environment* **2002**, *83*, 3–15.
10. Walker, J. J.; Beurs, K. M. de; Wynne, R. H.; Gao, F. Evaluation of Landsat and MODIS Data Fusion Products for Analysis of Dryland Forest Phenology. *Remote Sensing of Environment* **2012**, *117*, 381–393.
11. Martinuzzi, S.; Gould, W. a; Ramos Gonzalez, O. M.; Martinez Robles, A.; Calle Maldonado, P.; Pérez-Buitrago, N.; Fumero Caban, J. J. Mapping Tropical Dry Forest Habitats Integrating Landsat NDVI, Ikonos Imagery, and Topographic Information in the Caribbean Island of Mona. *Revista de biología tropical* **2008**, *56*, 625–39.
12. Hansen, M. C.; Roy, D. P.; Lindquist, E.; Adusei, B.; Justice, C. O.; Altstatt, A. A Method for Integrating MODIS and Landsat Data for Systematic Monitoring of Forest Cover and Change in the Congo Basin. *Remote Sensing of Environment* **2008**, *112*, 2495–2513.
13. Potapov, P.; Hansen, M. C.; Stehman, S. V.; Loveland, T. R.; Pittman, K. Combining MODIS and Landsat Imagery to Estimate and Map Boreal Forest Cover Loss. *Remote Sensing of Environment* **2008**, *112*, 3708–3719.
14. Martinuzzi, S.; Gould, W. a; Ramos Gonzalez, O. M.; Martinez Robles, A.; Calle Maldonado, P.; Pérez-Buitrago, N.; Fumero Caban, J. J. Mapping Tropical Dry Forest Habitats Integrating Landsat

- NDVI, Ikonos Imagery, and Topographic Information in the Caribbean Island of Mona. *Revista de biología tropical* **2008**, *56*, 625–39.
15. Wulder, M. a.; White, J. C.; Goward, S. N.; Masek, J. G.; Irons, J. R.; Herold, M.; Cohen, W. B.; Loveland, T. R.; Woodcock, C. E. Landsat Continuity: Issues and Opportunities for Land Cover Monitoring. *Remote Sensing of Environment* **2008**, *112*, 955–969.
 16. Cohen, W. B.; Goward, S. N. Landsat's Role in Ecological Applications of Remote Sensing. *BioScience* **2004**, *54*, 535.
 17. Dupas, C. A. SAR and Landsat TM Image Fusion for Land Cover Classification in the Brazilian Atlantic Forest Domain. *International Archives of Photogrammetry and Remote Sensing* **2000**, XXXIII , 96-103.
 18. Justice, C. O.; Vermote, E.; Townshend, J. R. G.; Defries, R.; Roy, D. P.; Hall, D. K.; Salomonson, V. V.; Privette, J. L.; Riggs, G.; Strahler, a. *et al.* The Moderate Resolution Imaging Spectroradiometer (MODIS): Land Remote Sensing for Global Change Research. *IEEE Transactions on Geoscience and Remote Sensing* **1998**, *36*, 1228–1249.
 19. Zhukov, B.; Oertel, D.; Lanzl, F.; Reinhackel, G. Unmixing-based Multisensor Multiresolution Image Fusion. *IEEE Transactions on Geoscience and Remote Sensing* **1999**, *37*, 1212–1226.
 20. Hilker, T.; Wulder, M. a.; Coops, N. C.; Linke, J.; McDermid, G.; Masek, J. G.; Gao, F.; White, J. C. A New Data Fusion Model for High Spatial- and Temporal-resolution Mapping of Forest Disturbance Based on Landsat and MODIS. *Remote Sensing of Environment* **2009**, *113*, 1613–1627.
 21. Hilker, T.; Wulder, M. a.; Coops, N. C.; Seitz, N.; White, J. C.; Gao, F.; Masek, J. G.; Stenhouse, G. Generation of Dense Time Series Synthetic Landsat Data Through Data Blending with MODIS Using a Spatial and Temporal Adaptive Reflectance Fusion Model. *Remote Sensing of Environment* **2009**, *113*, 1988–1999.
 22. Kalpoma, K. A.; Kudoh, J.; Member, A. Image Fusion Processing for IKONOS 1-m Color Imagery. *IEEE Transactions on Geoscience and Remote Sensing* **2007**, *45*, 3075–3086.
 23. Leckie, D. Advances in Remote Sensing Technologies for Forest Surveys and Management. *Canadian Journal of Forest Research* **1990**, *20*, 464-483.
 24. Helmer, E. H. H.; Amos, O. R.; Ópez, T. D. E. L. M. L.; Uñones, M. Q.; Iaz, W. D.; Service, U. F.; Box, P. O. Mapping the Forest Type and Land Cover of Puerto Rico, a Component of the Caribbean Biodiversity Hotspot. *Caribbean Journal of Science* **2002**, *38*, 165–183.
 25. Roy, D. P.; Ju, J.; Lewis, P.; Schaaf, C.; Gao, F.; Hansen, M.; Lindquist, E. Multi-temporal MODIS–Landsat Data Fusion for Relative Radiometric Normalization, Gap Filling, and Prediction of Landsat Data. *Remote Sensing of Environment* **2008**, *112*, 3112–3130.
 26. Holben, B. N.; Characterization of Maximum Value Composites from Temporal AVHRR Data. *Int. J. Remote Sensing* **1986**, *7*, 1417-1434.
 27. Huete, A.; Justice, C.; Leeuwen, W. MODIS Vegetation Index Algorithm Theoretical Basis Document ATBD13: http://modis.gsfc.nasa.gov/data/atbd/atbd_mod13.pdf.